Title: Maladaptation in cereal crop landraces following a soot-producing climate catastrophe

Authors: Chloee M. McLaughlin[1,3*], Yuning Shi[2], Vishnu Viswanathan[3], Lorne N. Leonard[2], Ruairidh Sawers[2], Armen R. Kemanian[2], Jesse R. Lasky[3,4*]

[1]Intercollege Graduate Degree Program in Plant Biology, Pennsylvania State University, University Park, PA 16802

[2]Department of Plant Science, Pennsylvania State University, University Park, PA 16802

[3]Department of Biology, Pennsylvania State University, University Park, PA 16802

[4]PAC Herbarium, Pennsylvania State University, University Park, PA 16802

*correspondence: cmc7333@psu.edu, lasky@psu.edu

Corresponding Author:

Classification: Biological Sciences (Evolutionary Biology)

Keywords: Crop modeling, genomic offset, genotype-environment associations, nuclear winter

(250) Abstract: Soot-producing global catastrophes such as nuclear war, super volcano eruption, or asteroid strike, although rare, pose a serious threat to human survival. Light-blocking aerosols would sharply reduce solar radiation and temperatures, decreasing crop productivity including for locally-adapted traditional crop varieties, i.e. landraces. Here, we test post-catastrophic climate impacts on four crops with extensive landrace cultivation: barley, maize, rice, sorghum, under a range of nuclear war scenarios. We used a crop growth model to estimate gradients of environmental stressors that drive local adaptation. We then fit genotype environment associations using high density genomic markers with gradient forest offset (GF offset) methods, and predicted maladaptation through time. As a validation, we found that our GF models successfully predicted local adaptation of maize landraces in multiple common gardens across Mexico. We found strong concordance between GF offset and disruptions in climate, and landraces were predicted to be the most maladapted across space and time where soot-induced climate change was the greatest. We further used our models to identify landrace varieties best matched to specific post-catastrophic conditions, indicating potential substitutions for agricultural resilience. We found the best landrace genotype was often far away or in another nation, though countries with more climatic diversity had better within-country substitutions. Our results highlight that a soot-producing catastrophe would result in the global maladaptation of landraces and suggest that current landrace adaptive diversity is insufficient for agricultural resilience in the case of the scenarios with the greatest change to climate.

(120) Significance statement: Extreme and sudden changes to climate would threaten traditional local crop populations adapted to historic climates, while the diversity present in crops may enhance agricultural resilience under changing climate. Here, we develop a framework to characterize current crop genotype-environment relationships, quantify maladaptation across space and time, and search for suitable varietal substitutions in the case of soot-induced climate change, such as in a nuclear winter. We find that a soot-producing catastrophic event would result in the global maladaptation of crop landraces and a suitable varietal substitution may not

exist for many locations. Our framework can be extended to understand the impacts of greenhouse gas induced climate change for plants adapted to historical local climates.

Introduction

Environmental variability due to changing climate poses one of the greatest threats to agricultural productivity (1). Increasingly, researchers aim to predict the effects of changing climate on agriculture, projecting constraints on crop production and anticipated decreases in yield (2, 3). For regions and crop species identified as vulnerable under future climates, strategies to increase agricultural resilience may include adapting management practices and substituting varieties or crop species (4).

A catastrophic incident is defined by the National Response Framework as, "any natural or manmade incident, including terrorism, that results in extraordinary levels of mass casualties, damage, or disruption severely affecting the population, infrastructure, environment, economy, national morale, and/or government functions". Soot-producing global catastrophic events, such as nuclear war, asteroid strike, or super-volcano explosion, are expected to produce significant climate change (5) through deflecting solar radiation, preventing sunlight from reaching the Earth's surface and causing global cooling. Since the spread of nuclear weapons during the twentieth century, there has been significant focus on assessing the consequences of a nuclear conflict on both society and the environment (6). Published climate models have been used to consider the impacts of nuclear wars on the growth of major grain crops (7–9) and summarize the degree to which the rapid environmental change induced by a soot-producing catastrophe would impact global crop production. To date, the impact of a soot-producing catastrophe on agricultural systems has not accounted for intraspecific diversity present in crop species, including landraces, and how this diversity may aid in increasing agricultural resilience. Cereal crops account for the most calories consumed by humans (10) and maintaining their production post-global catastrophe is of the utmost importance.

Crop landraces (local traditional varieties) contain most of the genetic diversity within many crops, much of which is not represented in modern breeding varieties (11) and are still widely cultivated in the developing world. The continual cultivation and selection of crops by farmers gives rise to these local varieties that often carry locally adapted alleles and phenotypes (12). Historically, landraces have contributed to plant breeding through the identification of traits and alleles for adaptation to stressful environments (water stress, salinity, and high temperatures) (13). Many thousands of landrace varieties are now stored in germplasm banks and represent untapped adaptive diversity that may increase agricultural resilience under changing environments (14).

The genetic basis of adaptation to local environments can be characterized through geographic associations between genotype and environment, known as genotype-environment associations (15). Genotype-environment associations have been used to study the adaptive potential of species (16), estimate optimal range shifts (17), and identify genes that may be advantageous for organisms under future climates (18). Genotype-environment associations may also give insights into which specific environmental pressures drive local adaptation (19–22). For landraces, a large portion of genomic variation can be explained by environments of origin (23–25), making them good systems for considering the environmental gradients driving local adaptation (26) and the geographic distribution of locally adapted alleles (27, 28).

An emerging approach for predicting adaptation to novel environments is first fitting genotype-environment models that describe how current allele frequencies change across environment under an assumption of local adaptation. Next, the fitted model is applied to a novel environment to determine the change in genomic composition required for adaptation to that environment, known as genomic offset (reviewed in (29)). The genotype-environment models

can further be extended to identify optimal genotypes or varieties for specific environments (25, 30) and guide movement of genotypes to minimize maladaptation to the novel climates. These models capture long-term signals of adaptation and may provide insights to genotypes that are the most vulnerable/sources of resilience to climatic variability (31).

We studied the climate impacts of a soot-producing catastrophe on broadly distributed globally important cereal crops for which landrace cultivation is important for smallholder farmers: *Sorghum bicolor* (sorghum), *Zea mays* (maize), *Oryza sativa* subsp. *indica* and *japonica* (rice), and *Hordeum vulgare* (barley). We used crop growth models to identify climate stressors and genomic models to estimate the degree of disruption to current landrace adaptation under several post-catastrophic scenarios differing in the amount of soot included in the climate model. We validated our genomic models through comparing predicted local adaptation and published maize landrace performance data collected in common gardens across diverse climates in Mexico. We further extended our genomic models to identify landrace varieties best matched to specific post-catastrophic conditions, supporting the management strategy of substituting vulnerable landrace genotypes for more resilient ones. There is a limited amount of research investigating the impacts of climate change on multiple species, potentially oversimplifying its effects on agricultural systems and ecosystems. Utilizing a multi-species approach allows us to confront this challenge, acknowledging the distinct impacts on various species that are vital for food production. For all crops included in this study, we find that landraces accessions with a distribution farther from the equator were most maladapted to post-catastrophic climates and were most often selected as the best varieties for substitutions. Further, methodology developed in this study may be extended to and prove valuable for understanding impacts of greenhouse gas induced climate change.

Results

Climate scenarios. We studied disruptions to current landrace adaptation for six nuclear war scenarios that simulate the impact of stratospheric soot on global climate (Fig. S1) using previously published weather forecast data (6, 32). The published weather files describe the climate impacts for five India-Pakistan nuclear war scenarios (soot injections of 5 Tg, 16 Tg, 27.3 Tg, 37 Tg, and 46.8 Tg), one United States-Russia scenario with a soot injection of 150 Tg, and a control run that describes normal fluctuations in climate.

Genotyped landrace accessions. To assess maladaptation in cereal crop landraces following a soot-producing catastrophe, we identified species for which landrace relatives are currently grown in the developing world that also had publicly available, high quality sequencing data of geographically diverse accessions. From these criteria, we selected four crop species: barley (n = 215), rice (n = 677 of the subsp. *indica,* n = 309 of the subsp. *japonica*), maize (n = 3,404), and sorghum (n = 1,779). The distribution of accessions covered most of the agricultural areas in the developing world (Fig. S2) across diverse climate regimes.

Using crop growth models to estimate integrated local climatic stressors under control and post-war conditions. Traditional implementations of genotype-environment associations typically use off-the-shelf climate parameters without connection to organismal biology and without consideration of phenology. However, actual climate-driven stress likely emerges from a combination of conditions (e.g. precipitation and temperature) and depends on organismal phenology and development. To address these issues, we used the agroecosystem model, *Cycles*,

to simulate growth and stress parameters for our full set of genotyped, georeferenced landrace accessions (n = 6,384) under control and six nuclear war conditions that differ in the quantity of stratospheric soot simulated (5 Tg, 16 Tg, 27 Tg, 37 Tg, 47 Tg, 150 Tg). *Cycles* simulations selects a planting date when the climate of the input conditions are suitable for the specific crop, and simulates crop growth until the time of harvest or termination, using parameters specific to each of our four species.

We used *Cycles* outputs to infer emergent climatic, growth, and stress values experienced during key phenological stages of crop, constrained to the growing period for each simulated accession (Table S1). Thus, the selected model outputs characterized differences in climate and potential stress experienced by a given landrace accession under control and post-war target climates. For each climate scenario and accession, we extracted 13 variables representative of average temperature, coldest temperature, water stress, and solar radiation experienced by simulated landrace accessions across the vegetative, reproductive, and total growth and days to reach maturity (Fig. 1). While in reality landrace accessions likely exhibit variation in response to environment, modeling this genetic variation was not our goal at this stage. Rather, our goal was to use *Cycles* estimate integrative climate stressors through space and time.

As previously described, in all war scenarios regardless of detonation location, produced soot spreads globally and causes disruptions to solar radiation reaching the earth's surface, resulting in global cooling (6, 32). Stratospheric soot from each post-war scenario dissipated over the course of a decade and the climate anomalies caused by atmospheric soot decreased proportionally, with respect to severity of the scenario. Across all scenarios, shortwave radiation reached its all-time low two years post-war, corresponding to the point at which *Cycles* modeled crops were simulated with the lowest average solar radiation (Fig. 1). Consequently, global

surface temperature immediately and rapidly declined after the catastrophe and on average reached its lowest point in the third year post-war, with more extreme cooling in the Northern Hemisphere (6, 33). Our crop models summarized this cooling trend. Daily average temperature for landraces modeled by *Cycles* reached its lowest point two to three years post catastrophe. Barley, our crop with a primary distribution in the Northern Hemisphere, experienced the coolest post-war temperatures (Fig. S2; Fig. 1). In the coolest year of the 150 Tg Russia-US scenario, average temperature of the growing season across all simulated accessions decreased by 10 °C for maize and sorghum, 14 °C for rice subsp. *japonica*, 16 °C for rice subsp. *indica*, and 20 °C for barley, indicating the severity of this scenario.

For maize, rice, and sorghum, whose landraces modeled in this study were mostly tropical, declines in temperature across the simulated growing season without a gain in solar radiation led to an increase in the number of days required for a plant to reach maturity. The strength of this relationship increased with the more severe soot scenarios (Fig. S3). In our simulations, failure to accumulate enough thermal time during the growing season was recorded as the crop not reaching maturity. As *Cycles* does not account for genetic variation among landraces, an individual not projected to reach maturity can be interpreted as a climate that is relatively inhibitory for growth. The simulated number of days to maturity generally corresponding to the severity of the climate anomaly of the post-war soot scenario. The most extreme environmental effects of the 150 Tg scenarios at least doubled the number of days to reach maturity for all tropical crops (Fig. 1). In the second post-war year of this scenario, 90% of barley, 62% of rice subsp. *indica*, 51% of rice subsp. *japonica*, 54% of maize, and 33% of sorghum accessions were projected to not reach maturity.

Identification of environmentally adaptive genetic loci. For each crop species, we acquired published genotype data of landraces used in *Cycles* simulations above. The final set included 6,384 accessions: 215 barley accessions with exome sequencing (1,688,807 SNPs) (Russell et al., 2016), 3,404 maize accessions with genotyping-by-sequencing (GBS) (946,072 SNPs) (Romero Navarro et al., 2017), 986 rice accessions with whole genome resequencing (WGS) (677 subsp. *indica*, 309 subsp. *japonica*; 9.78 million SNPs) (Gutaker et al., 2020), and 1,779 sorghum accessions with GBS (459,304 SNPs) (Hu et al., 2019). All genotype files were converted to BED format and processed in PLINK (Purcell et al., 2007).

To build models predicting maladaptation in crop landraces following change in climate post-war, we first identified a subset of genomic loci that we hypothesized were more likely to underly local adaptation. Specifically, we identified climate-associated loci and phenology quantitative trait loci (QTL) for use in models that summarize current genotype-environment associations. Following methods described in (34) and for each crop species, we used partial redundancy analysis (pRDA) to identify the top 1,000 genetic loci associated with variation in 13 *Cycles* environmental variables under the control scenario (Fig. S4). To ensure potentially critical phenology QTL were accounted for in our models, we further identified single nucleotide polymorphisms (SNPs) of loci found within and +/- 5kb of known flowering time network genes (Table S2). We identified loci known to be involved in flowering time for each crop species by literature review, obtained gene coordinates for each gene, and extracted all SNPs that overlapped within and +/- 5kb around the genomic region. The number of flowering time SNPs included in our genomic offset models for each of our focal species included 865 for barley, 1,605 for rice subsp. *indica*, 884 for rice subsp. *japonica*, 888 for maize, and 176 for sorghum (differences in number are a product of market density). In total, the final genetic dataset used to

build each species' genomic offset model included the top 1,000 SNPs associated with variation in *Cycles* environmental parameters identified by pRDA and the flowering time SNPs.

Control scenario GF models describe existing genome-environment associations. We built gradient forest models (GF) representative of current genotype-environment associations using the loci mentioned above and control *Cycles* environmental parameters for each crop species. GF is a nonparametric multivariate approach that fits an ensemble of regression trees using Random Forest (35) and models changes in allele frequency along environmental gradients (36). GF's functions provide a means to rescale environmental predictors from their normal units (e.g., °C, mm) into a unit of cumulative importance for describing variation in a genetic dataset. For all GF models, the emergent environmental parameter of simulated days to maturity was in the top five most important predictors for describing variation in the putatively adaptive genomic loci (Fig. S5). No single environmental variable was substantially more related to allele frequencies of these loci, indicating that GF models captured genome-wide relationships to multiple environmental gradient signals rather than a high impact at a single locus (31). The differing importance of environmental variables specific to a growth stage of plants (variable constrained to the vegetative or reproductive stage of growth) indicated that stress experienced by plants changes across the different phenological stages of growth and genetic variation can be associated with life-stage specific stress.

GF models capture adaptation in landraces. To test if GF models captured current environmental adaptation in landraces, we compared published performance data of 11,762 maize landraces grown across 13 common gardens in Mexico (28, 37) to GF predicted genotype-

environment relationships using *Cycles* parameters of the control scenario. The common gardens spanned geographic and environmental range of maize cultivation (Fig. S6). To predict adaptation, we calculated GF offset for each accession in each common garden as the Euclidian distance between the accession's control GF modeled genotype-environment association and the expected genomic composition at the common garden. As offsets are calculated from current genotype-environment relationships in the GF models, they are weighted by the contribution of different loci that are involved in current landrace adaptation and indicate what amount of genetic change would be required for adaptation to a common garden. Accessions with a low GF offset are expected to be better adapted to the conditions at the common garden. We found that, indeed, accessions performed best (height and yield measures) in sites where they had low GF offset (Fig. 2A; Fig. S5B). Furthermore, anthesis silking interval (ASI, synchronicity of male and female flower maturity) was reduced when accessions were grown at sites for which they had lower GF offset. ASI is a reliable predictor of stress in maize (38), indicating plants were less stressed when grown in common gardens to which they are predicted to be adapted (lower GF offset).

The degree of GF offset post-catastrophe follows the magnitude of climate disruption. We used the fitted GF models to predict the expected locally-adapted genomic composition for landraces across space and time under the six post-war scenarios. To predict the magnitude of maladaptation, we calculated GF offset as the Euclidian distance between a given landrace source location's expected genomic composition between control and the soot scenarios. High GF offset values corresponded to a greater degree of maladaptation and represent a greater shift in allelic composition required for adaptation to the future environment. For all crops and

scenarios, GF offset values followed the trend in post-war climate disruptions, with a sharp increase and gradual recovery after 10 to 15 years (Fig. 2B-F; Fig. S7). GF offset for all crops reached its highest point two to three years post-catastrophe, indicating that crops were expected to have the highest degree of maladaptation when global solar radiation and temperatures reached their all-time low. Maximum GF offset of each target scenario linearly corresponded to the amount of soot simulated (Fig. 2 B-F). Across all crop species, we detected a strong latitudinal pattern associated with GF offset values, equatorial regions which experienced less adverse climate impacts were predicted to be less maladapted to post-war conditions (Fig. 3).

Identification of landrace substitutions for post-catastrophe adaptation. We leveraged our GF models to identify landrace genotypes best matched to specific post-catastrophic conditions, indicating potential varietal substitutions for locations with landraces that were the most maladapted to post-catastrophic climates. Under post-catastrophic conditions, many locations will not have climate suitable for the cultivation of crops and we constrained our analyses to only look for substitutions for locations that were projected to have a crop reach maturity in the worst year (year 2 post-strike) of the 150 Tg scenario. After filtering for locations that were not expected to be suitable for agriculture, 10% of barley, 38% of rice subsp. *indica*, 49% of rice subsp. *japonica*, 46% of maize, and 67% of sorghum landraces source locations were retained to search for a suitable substitution. For the remaining locations, we identified the most vulnerable locations as those with the highest GF offset. We then searched for the most optimal substitution globally as well as the best within country substitution, identifying the landrace accession with the lowest GF offset to the post-catastrophic climate in the vulnerable location (Fig. 5).

Across all crops, the most optimal substitution was often far away (~1000 to ~10,000 km) and across country borders. For many locations, the best substitution still had a high degree of GF offset, indicating that there was not a genotype that was expected to be adapted to the post-catastrophic climate at the vulnerable location included in our dataset (Fig. 5A, C, E, G, I). This could be due to the severity of the novel climate at the vulnerable location, the absence of a landrace accession that was expected to be adapted to the novel environment, or some combination of both. For all crops, the best substitution trajectories typically moved landrace accessions from poles and high elevations towards the equator and low elevations, indicating that germplasm adapted to currently cooler climates may be sources of resilience for locations that are still expected to support agriculture post-catastrophe. For all crop species, there were instances where one genotype was the most optimal substitution for multiple vulnerable locations, suggesting particularly valuable genotypes.

In the case of a catastrophe, substitutions across long distances may not be possible due to socioeconomic disruptions, e.g. in transport and trade. We further searched for the optimal within-country substitution. For all crops, within country substitutions with a low GF offset were rare; within country substitutions always had a higher GF offset, corresponding to higher expected maladaptation, than the optimal global substitution (Fig. 5B, D, F, H, J). Though maintaining a high degree of maladaptation, most within country substitutions included trajectories moving individuals towards the equator and lower elevations.

The within-country current diversity of environments to which landraces are adapted may be important for finding suitable substitution. To test this hypothesis, we compared the GF offset for the 25% most maladapted locations within each country after using global substitutions versus within-country substitutions. We focused on sorghum because it was the crop with the

most countries having viable cultivation in year 2 of the 150 Tg scenario, giving power to compare countries. As expected, all 31 countries with at least 5 sorghum accessions had greater GF offset for the most maladapted locations when only using within-country substitutions, compared to the global substitutions. The proportional inferiority of within-country compared to global substitutions was only weakly related to the number of landraces from each country ($r = 0.27$, $p = 0.14$). We next tested if the control climate mean and variance influenced the inferiority of within-country substitutions in a multiple regression, while accounting for the number of landraces in each country. We found that the countries with less variance among landraces in cold stress and greater mean cold stress had significantly worse within-country substitutions compared to global (linear model, mean cold $t = 3.99$ $p = 0.0005$, variance in cold $t = 2.54$ $p = 0.0173$, number of landraces $t = 0.37$ $p = 0.7173$, $R^2 = 0.45$). This highlights the potential future value of diversity for regions and nations housing landraces adapted to diverse climates.

Discussion

The resilience of agricultural systems to changing climate determines global food security. In this study we used information on landrace genetic variation and environment of origin for agronomically important cereal crops to predict disruptions to their adaptation/cultivation and to explore if the diversity of landraces may be beneficial sources of resilience in the case of a soot-producing climate catastrophe. Consistent with other groups who have investigated the consequences of a soot-producing catastrophe on global agriculture (7, 9) and fisheries (33), we find the climate impacts would be devastating to global subsistence agriculture, many locations would become unsuitable for agriculture, and the locations that

remain suitable may not have sufficient local landrace diversity within a species to enable a successful substitution of a resilient variety.

Our crop model results correspond to previous estimates of the climate impacts of soot-producing catastrophes (6, 7, 9, 32, 33, 39) while also providing an assessment of the diversity of environments to which crop landraces of globally important cereal crops are adapted. Increases in the number of days simulated to reach maturity corresponded to the climate anomalies of reduced daily temperature and solar radiation. In the years and locations with the greatest climate impacts, landraces in higher latitudes rarely achieved full maturity. Colder temperatures have a direct impact on crop growth by slowing down the process of phenological development, diminishing photosynthetic activity and potentially causing tissue damage.

We built GF models to summarize current landrace genotype-environment relationships and validated that GF models captured real adaptive differences through use of phenotypic data collected for a broad diversity panel of maize landraces grown in common gardens across Mexico. We show that predicted maladaptation, in the form of GF offset, is associated with height, yield, and stress-related traits, demonstrating a new test of these tools (24, 40). Landrace accessions had classic phenotypic patterns of local adaptation when grown in common gardens they had a low degree of maladaptation to (low GF offset), suggesting GF models captured broad adaptation of landraces' local environments (41). However, landrace performance was not perfectly predicted by our genotype-environment model. This inability to completely predict adaptation may be attributable to limitations of GEA approaches or to the maintenance of diversity within environments, though our GF model identifies a single optimal genotype for each environment. In general, reciprocal transplants and common gardens often find mixed evidence for local adaptation (42). Genotypes from the same environment may differ in

performance in a given common garden environment if processes like migration or environmental fluctuations maintain diversity within populations or if important selective forces are not present in experimental conditions. Our validation methodology confirms that GF offset can be a powerful tool to capture current genotype-environment relationships though our inability to perfectly predict adaptation likely highlights a potential importance of maintaining genetic diversity within a site.

When environments change and populations are not able to track the environmental change through plasticity or rapid shifts in genetic composition, populations may become maladapted and have reduced fitness in a novel climate (43). In our case, landraces were predicted to be the most maladapted, or have the highest GF offset, in the locations where climate was the most disrupted from long-term averages, corresponding to the most extreme soot scenarios and the years post-war where atmospheric soot was the most abundant. The strong relationship we observed between GF offset and soot-induced change in climate is perhaps unsurprising. GF models are trained using current genotype-environment associations and any shift in the environment will likely require a change in genomic composition to track adaptation to a novel climate. The ability to interpret the magnitude of offsets derived from GF-derived functions in an ecologically meaningful way has recently become a point of discussion. Genetic-based quantifications of adaptation (34) and offset (44) can be biased for unsampled areas or if the projected environment exceeds what is used to train the model. Though we have a broad sampling of landrace accessions for each focal crop species that are adapted to a diversity of environments and used in GF genotype-environment models, the extremeness and novelty of post-war climates used in this study likely make predicting maladaptation difficult (45). At the same time, though the true magnitude of maladaptation may be difficult to quantify, our GF

models allow us to incorporate measures of climate-associated genomic variation for the identification of the most vulnerable locations that will likely require a varietal substitution.

Crop diversity has been suggested as a potential solution to mitigate climate impacts on agriculture (25, 46). We found that most substitutions that were well matched to vulnerable locations required long migration distances and for many locations, a landrace adapted to the novel environment at the vulnerable location does not exist within our dataset (25). Substitutions that maintained a high level of GF offset indicated landrace varieties that may remain maladapted to the novel climate, and no other varieties were better adapted to the vulnerable, tested location. At the same time, for locations where the cultivation of crops remains possible, the identification of multiple suitable genotypes may be important for the maintenance of crop diversity within a site. For vulnerable locations that were not predicted to have a well-adapted substitution, switching cultivation from to faster-maturing crop varieties, or other non-cereal crop species that tolerate lower temperatures (e.g. potato)(47), may be a strategy for increased resilience. However, the adoption of a new crop species requires a significant investment by farmers and substantial modifications of farmer and consumer behavior (48).

Though our study highlights maladaptation in cereal crop landraces following a soot-producing catastrophe, methodology used in this study can also be leveraged to understand disruptions to adaptation and possible genotype substitutions (also known as assisted gene flow) given any change in climate, including greenhouse gas induced climate change (49). Our results indicate that for the most populations most vulnerable to climate catastrophe, the plant genetic diversity within a country may not be sufficient for resilience and substitutions across country borders of further distances may be required.

Methods

We used landraces to characterize global disruptions to adaptation and identify resilient accessions in the case of a climate catastrophe that produces soot (Fig. S1). Selected landrace crop species fulfilled two criteria - 1. Landrace relatives of the species account for a large portion of accessions currently grown and 2. High quality sequencing data of geographically diverse accessions were publicly available. From these criteria, we selected four cereal crop species- *Hordeum vulgare* (barley), *Oryza sativa* (rice) subsp. *indica* and *japonica*, *Zea mays* (maize), and *Sorghum bicolor* (sorghum). For all analyses, the rice subsp. *indica* and *japonica* were run separately. Altogether, selected focal crop species cover most of the agricultural areas of the globe (Fig. S2) and are cultivated in and adapted to diverse climate regimes.

Weather data. Previously published weather data described in Toon et al., (2019) and Coupe et al., (2019) simulate the climate impacts of India-Pakistan and US-Russia wars using the Community Earth System Model (CESM, version 1.3) with the Whole Atmosphere Community Climate Model Version 4 (WACCM4, version 4) as the atmospheric component, or CESM-WACCM4 (Marsh et al., 2013). The climate impacts of nuclear war were simulated by injecting varying quantities of black carbon (soot) into the stratosphere in a layer between 100 and 300 hPa over a 1-week period starting on 15 May in year 5 of the simulation above the U.S. and Russia, or the South Asian subcontinent (Bardeen et al., 2021; Coupe et al., 2019; Toon et al., 2019). In total, six nuclear war scenarios were simulated, and we refer to the year soot was injected as year "0". For the five India-Pakistan nuclear war scenarios (soot injections of 5 Tg, 16 Tg, 27.3 Tg, 37 Tg, and 46.8 Tg, representing a range of arsenal sizes) simulations were each

run for 19 years. One United States-Russia scenario with a 150 Tg soot injection was also considered, and the simulation was run for 21 years. This scenario assumes both countries use most of their nuclear arsenals (Robock et al., 2007) and is still possible given modern nuclear arsenals. Additionally, a control run that begins in the year 2000 and simulates normal atmospheric circulations was run for 20 years (Coupe et al., 2019; Toon et al., 2019).

Cycles. The agroecosystem model *Cycles* was used to simulate growth and stress parameters of landrace accessions' point of origin using conditions accessions are expected to be adapted to (control scenario) and post-catastrophe conditions (six target post-nuclear war scenarios). *Cycles* is a process-based multi-year and multi-species agroecosystem model (Kemanian et al., 2022) that requires a number of input files to simulate crop growth. All simulations were carried out using Cycles v0.13.0 (https://github.com/PSUmodeling/Cycles). The crop description file defines the physiological and management parameters that control the growth and harvest of crops used in the simulation. For each of our crop species, we used a Cycles default crop parameters from the default crop description file. The management (operation) file defines the daily management operations to be used in a simulated crop rotation. We activated conditional planting where Cycles "plants" a simulated crop once certain soil moisture and temperature levels are satisfied within a window of planting dates. For many of the scenarios where planting conditions are not met (i.e. daily temperature remains too low) Cycles forced planting on the last day of the planting window. We turned on the automatic nitrogen fertilization option and set planting density to 67% for all crops in the simulation to be grown without nitrogen limitations so that stress observed in model outputs was due entirely to climatic factors. Weather files were built using the CESM-WACCM4 outputs as described Toon et al., (2019) and Coupe et al., (2019) for

control and six target post-nuclear scenarios, formatted for use in Cycles. The weather files were generated by aggregating the three-hourly CESM output to daily time steps at all CESM grids, which have a 1.9° latitude × 2.5° longitude resolution. Weather files were matched to landrace point of origin for each simulated accession, where the climatic parameters used to simulate growth match the location accessions were sourced from. Weather files included variables describing difference in daily precipitation, temperature, solar radiation, humidity, and wind. Soil physical parameters were obtained from the ISRIC SoilGrids global database (Hengl et al., 2015) via the HydroTerre data system (Leonard & Duffy, 2016, 2013, 2014) for all simulation locations. Soil files were also matched to landrace point of origin for each simulated accession and describe the average soil characteristics and land use for crop cultivation types. For accessions designated as paddy rice by (Gutaker et al., 2020) we used the irrigated or post-flooding land use type. Rainfed land use type was used for all other simulated crop accessions.

For all simulated accessions of each crop species, seven Cycles simulations, including the control scenario and six target scenarios were performed separately. Cycles models simulated 20 years of crop growth for the control scenario, 15 years of crop growth after impact for the India-Pakistan scenarios (5 Tg, 16 Tg, 27 Tg, 37 Tg, 47 Tg, and 150 Tg), and 17 years of crop growth for the US-Russia scenario (150 Tg). From the outputs of each Cycles simulation and for each year growth was simulated, we extracted values summarizing the environmental stress and simulated growth plants experienced for each of our focal crop species. Variables included information on the number of days to reach maturity, water stress, cold stress, and light stress experienced across simulated plant growth and when in the vegetative and reproductive phase. For accessions not projected to reach maturity, certain environmental summary variables were

not extractable, and we imputed the 95% stress of the variable for each accession with missing environmental values, specific to crop species and each year growth was simulated for.

Genotyped datasets. For each landrace species, raw genotype files were filtered for minor allele frequency (MAF) removing all SNPs with lower than 5% MAF and for linkage disequilibrium (LD) to reduce the number of SNP candidates we tested for environmental association. As the initial genotype files differed in size, the LD filter step included different conditions to thin files. We used --indep-pairwise 30 10 .1 for both rice subsp. (indica and japonica) and sorghum, and --indep-pairwise 100 10 .05 for the maize and barley data files. This filtering step resulted in 74,430 SNPs for barley, 43,818 SNPs for rice subsp. japonica, 61,430 SNPs for rice subsp. indica, 67,522 SNPs for maize, and 20,387 SNPs for sorghum to test for association to Cycles environmental parameters.

Genome scan for environmentally related SNPs. Genotype-environment associations test for genetic variation that is statistically correlated to environmental predictors. We followed partial redundancy analysis (pRDA) methods developed by Capblancq & Forester (2021) to identify loci putatively involved in environmental selection for our focal crop species. For each crop species, pRDA models were built using population allele frequencies (population defined as accessions from the same geocoordinates) from the filtered genetic dataset as response variables and 13 averaged environmental variables from 20 years of simulated Cycles growth under the control conditions as explanatory variables. Neutral genetic structure was accounted for by including the first three axes of a population PCA as conditional covariables. Using the *rdapat* function described in Capblancq et al., (2018), we identified the top environmentally related

(outlier) loci based on the extremeness of their loading along a Mahalanobis distance distribution calculated between each marker and the center of the first two RDA axes. P-values for each marker were derived as this distance, corrected for the inflation factor using a chi-squared distribution with two degrees of freedom. We then selected the top 1,000 markers with the lowest P-values as candidate outliers to represent putative loci involved in environmental adaptation. The analysis was carried out using R/vegan (Oksanen et al., 2022).

Identification of flowering time SNPs. We further accounted for genetic variation involved in plant phenological processes by including SNPs of known flowering time network loci for each focal crop species. We conducted a literature search to identify genes known to be involved in the flowering time network for each crop (Table S1). Gene coordinates of each flowering time gene were gathered from the gff3 files that corresponded to each reference genome used to call SNPs. For maize, rice subsp. *indica* and *japonica*, and sorghum we also included SNPs found +/- 5 kb of each flowering time locus to account for variation in cis-regulatory elements. Barley sequence information was reported as contigs and we extracted SNPs located in contigs previously identified to overlap with homologs of well-characterized genes in *Arabidopsis thaliana* (Russell et al., 2016). Gene coordinates for the location of each flowering time gene region or flowering time related contig extracted using --extract in PLINK (Purcell et al., 2007).

Gradient forest models and calculation of offset. Gradient forest (GF) is a machine learning algorithm extended from random forest which searches for genotypic patterns as associated with environmental descriptors. Using R/gradientForest::gradientForest (Ellis et al., 2012), we built GF models to associate current adaptive allelic diversity (combined environmentally related and

flowering time network genetic dataset) with Cycles environmental descriptors from the control simulation, averaged across the 20 years of modeled growth (hereafter, control GF). Models were built separately for each of our focal crop species to describe control genotype-environment relationships. The control GF model parameters were tuned to increase the number of trees built to *ntree* = 500.

Genomic offset (also known as genomic vulnerability) is one metric used to characterize maladaptation with a genomic context (reviewed in Rellstab et al., 2021). The distance between current and expected genotype-environment associations under some change in environment is representative of the genomic offset, or the genetic shift required in a population to adapt to the future climate. Comparing control genotype-environment associations captured by GF models, and projected genotype-environment for different scenarios (common garden, target scenarios, vulnerable locations) we made several measurements of GF offset to summarize predicted maladaptation. For all GF offset calculations, we followed methods described in Rhoné et al. (2020). To validate that our GF models captured current genotype-environment associations, we first used the maize control GF model to predict the genomic composition expected at common gardens maize landraces had been phenotyped in for a previous study (Romero Navarro et al., 2017). Here, the GF offset was defined as the Euclidean distance of current genotype-environment relationships at the common garden site from the genotype-environment relationship of each landrace's point of origin. This measure summarized how genetically well matched a landrace was to the common garden it was grown in (measure of predicted maladaptation to a common garden) and was compared to the phenotypic breeding values for each landrace grown in a common garden.

Validation of gradient forest-predicted adaptation. We used phenotypic data of maize landraces grown in 23 trials across 13 common garden locations over 2 years to confirm that our control GF models captured real differences in current landrace genotype-environment relationships. We restricted our analysis to include the phenotypic data of landraces accessions that were simulated in Cycles models.

Briefly, phenotyped accessions are a part of the broader SeeD evaluation of the maize landrace collection (Romero Navarro et al., 2017). Accessions were planted in multiple environments under a replicated F1 crossing. Importantly, two features of the crossing design ensure that phenotype data is not overly biased by elevational adaptation. Crossed plants were preferentially grown in locations that were of similar adaptation (highland tropical, sub-tropical or lowland tropical) to their home environment and each plant was crossed to a tester that was adapted to the environment that the F1 seeds were grown in. These design features allowed for comparison of a larger sample of accessions, but also led to an unbalanced experimental design. As a further consequence of the experimental design, apparent adaptive differences among landraces may be reduced and make phenotypic estimates of adaptation more conservative (Gates et al., 2019). We extracted phenotypic information capturing differences in plant height (PH), the total weight of ears (kernels and cob) measured in the field (field weight; FW), bare cob weight (BCW), moisture adjusted grain weight per hectare (GWH), days to anthesis (DA), days to silking (DS), and anthesis-silking interval (ASI) for plants grown in trials (https://data.cimmyt.org/dataset.xhtml?persistentId=hdl:11529/10548233). The phenotypic datasets ranged from having n = 4,851 (BCW) to n = 11,762 (ASI) across the field sites. Following methods from Gates et al., (2019) and Romero Navarro et al., (2017), we estimated

breeding values controlling for tester, checks, and field position in a complete nested model. We further accounted for the random effect of tester and year.

Calculation of offset under post-catastrophic conditions. Once we confirmed that our maize control GF model captured phenotypic differences representative of adaptation to common gardens with conditions most like the source locations landraces were adapted to, we extended our control GF models to predict maladaptation in crop landraces under the six post-war target climate scenarios. Here, GF offset was calculated as the Euclidian distance between the current predicted genotype-environment relationships and future projected genotype-environment relationships across all 13 Cycles summary environmental descriptors.

We confirmed that offset values were correlated to relative changes in environment that were most related to genotype-environment relationships summarized by the control GF model by comparing the difference in GF offset (target subtracted from control) versus the change in climate where environmental variables were scaled and adjusted by their relative contribution to GF models (Fig. S8).

Identification of landrace substitutions for post-catastrophe adaptation. To understand if existing landrace diversity may be a source of resilience following a climate catastrophe, we used our GF models to identify the best suited substitutions for locations with the landraces that are the most maladapted (Caproni et al., 2023; Rhoné et al., 2020) under the most extreme target scenario (150 Tg) and for the year where climate is the most disrupted (post-strike year 2). We first excluded all locations not predicted to reach maturity, so as not to identify substitutions to locations where agriculture would not likely be possible. For the remaining locations, we defined

the most vulnerable locations as those with the highest GF offset to search for the most optimal and the best within country substitution. Clusters of vulnerable pixels were identified using R/DBscan::dbscan (Hahsler et al., 2019), which groups pixels based off proximity. Clustering was based on the geographic distance between vulnerable pixels measured with R/geosphere::distm (Hijmans et al., 2022). Only clusters separated by <1000 km were retained for further analysis.

For each vulnerable cluster, a GF offset (i.e., Euclidean distance) was calculated between the projected genotype-environment relationship of the vulnerable location under the 150 Tg target scenario and the control GF modeled genotype-environment relationship across all landrace accessions included in the model. The lowest GF offset was defined as the minimum Euclidean distance and identified the current landrace accession predicted to be best adapted to the future climate condition of the vulnerable area. For accessions that were not perfectly adapted to the locations they were substituted to (i.e GF offset is higher than 0), this measure represented the genomic gap that still needs to be filled for the migrated varieties to be fully adapted to their new location and conditions (assuming current genotype-environment relationships are representative of prefect adaptation). High GF offset indicated substitutions where accessions are not predicted to be well adapted to the locations they were substituted to, and no other landraces included in the model were better adapted to the projected climate of the vulnerable area.

Acknowledgments and funding sources

We thank Liana Burghardt and Estelle Couradeau for comments on earlier versions of this manuscript. We would like to thank Daniel Runcie and Jeffrey Ross-Ibarra for helpful feedback on analyses using the common garden data. We would also like to thank the Penn State Food Resiliency team for input and discussion. This research was supported by the Food Resilience in the Face of Catastrophic Global Events grant funded by Open Philanthropy.

Author contributions

C.M.M., Y.S., A.K., J.R.L designed research; C.M.M. performed research; Y.S., L.L., A.K. contributed new analytic tools; C.M.M. and J.R.L. analyzed data; C.M.M. wrote the manuscript, with input from L.L., Y.S., A.K., R.J.H.S., and J.R.L.; All authors contributed to manuscript revision.

References

1. T. Lemi, Effects of Climate Change Variability on Agricultural Productivity. *IJESNR* **17** (2019).

2. C. O. Stöckle, *et al.*, CropSyst model evolution: From field to regional to global scales and from research to decision support systems. *Environmental Modelling & Software* **62**, 361–369 (2014).

3. T. Van Klompenburg, A. Kassahun, C. Catal, Crop yield prediction using machine learning: A systematic literature review. *Computers and Electronics in Agriculture* **177**, 105709 (2020).

4. M. A. Altieri, C. I. Nicholls, A. Henao, M. A. Lana, Agroecology and the design of climate change-resilient farming systems. *Agron. Sustain. Dev.* **35**, 869–890 (2015).

5. R. P. Turco, O. B. Toon, T. P. Ackerman, J. B. Pollack, C. Sagan, Nuclear Winter: Global Consequences of Multiple Nuclear Explosions. *Science* **222**, 1283–1292 (1983).

6. J. Coupe, C. G. Bardeen, A. Robock, O. B. Toon, Nuclear Winter Responses to Nuclear War Between the United States and Russia in the Whole Atmosphere Community Climate Model Version 4 and the Goddard Institute for Space Studies ModelE. *Journal of Geophysical Research: Atmospheres* **124**, 8522–8543 (2019).

7. J. Jagermeyr, *et al.*, A regional nuclear conflict would compromise global food security. *Proceedings of the National Academy of Sciences of the United States of America* **117**, 7071–7081 (2020).

8. M. Özdoğan, A. Robock, C. J. Kucharik, Impacts of a nuclear war in South Asia on soybean and maize production in the Midwest United States. *Climatic Change* **116**, 373–387 (2013).

9. L. Xia, *et al.*, Global food insecurity and famine from reduced crop, marine fishery and livestock production due to climate disruption from nuclear war soot injection. *Nat Food* **3**, 586–596 (2022).

10. D. Lafiandra, G. Riccardi, P. R. Shewry, Improving cereal grain carbohydrates for diet and health. *Journal of Cereal Science* **59**, 312–326 (2014).

11. M. A. Azeez, A. O. Adubi, F. A. Durodola, Landraces and Crop Genetic Improvement. *Intech* **i**, 13 (2016).

12. T. C. C. Villa, N. Maxted, M. Scholten, B. Ford-Lloyd, Defining and identifying crop landraces. *Plant Genetic Resources* **3**, 373–384 (2005).

13. S. L. Dwivedi, *et al.*, Landrace Germplasm for Improving Yield and Abiotic Stress Adaptation. *Trends in Plant Science* **21**, 31–42 (2016).

14. D. Hoisington, *et al.*, Plant genetic resources: What can they contribute toward increased crop productivity? *Proceedings of the National Academy of Sciences of the United States of America* **96**, 5937–5943 (1999).

15. J. R. Lasky, E. B. Josephs, G. P. Morris, Genotype–environment associations to reveal the molecular basis of environmental adaptation. *The Plant Cell* (2022). https://doi.org/10.1093/plcell/koac267.

16. M. Vanhove, *et al.*, Using gradient Forest to predict climate response and adaptation in Cork oak. *Journal of Evolutionary Biology* **34**, 910–923 (2021).

17. P. Sklenář, A. Kučerová, J. Macková, K. Romoleroux, Temperature Microclimates of Plants in a Tropical Alpine Environment: How Much does Growth Form Matter? *Arctic, Antarctic, and Alpine Research* **48**, 61–78 (2016).

18. M. C. Fitzpatrick, S. R. Keller, Ecological genomics meets community-level modelling of biodiversity: Mapping the genomic landscape of current and future environmental adaptation. *Ecology Letters* **18**, 1–16 (2015).

19. J. R. Lasky, *et al.*, Characterizing genomic variation of Arabidopsis thaliana: The roles of geography and climate. *Molecular Ecology* **21**, 5512–5529 (2012).

20. O. Razgour, *et al.*, Considering adaptive genetic variation in climate change vulnerability assessment reduces species range loss projections. *Proc. Natl. Acad. Sci. U.S.A.* **116**, 10418–10423 (2019).

21. O. Savolainen, M. Lascoux, J. Merilä, Ecological genomics of local adaptation. *Nat Rev Genet* **14**, 807–820 (2013).

22. J. Stapley, *et al.*, Adaptation genomics: the next generation. *Trends in Ecology & Evolution* **25**, 705–712 (2010).

23. R. M. Gutaker, *et al.*, Genomic history and ecology of the geographic spread of rice. *Nature Plants* **6**, 492–502 (2020).

24. J. R. Lasky, *et al.*, Genome-environment associations in sorghum landraces predict adaptive traits. *Science Advances* **1**, 1–14 (2015).

25. B. Rhoné, *et al.*, Pearl millet genomic vulnerability to climate change in West Africa highlights the need for regional collaboration. *Nature Communications* **11** (2020).

26. C. M. McLaughlin, *et al.*, Evidence that variation in root anatomy contributes to local adaptation in Mexican native maize. *Evolutionary Applications* **17**, e13673 (2024).

27. E. S. Bellis, *et al.*, Genomics of sorghum local adaptation to a parasitic plant. *Proceedings of the National Academy of Sciences* **117**, 201908707 (2020).

28. D. J. Gates, *et al.*, Single-gene resolution of locally adaptive genetic variation in Mexican maize. *bioRxiv* 706739 (2019). https://doi.org/10.1101/706739.

29. C. Rellstab, B. Dauphin, M. Exposito-Alonso, Prospects and limitations of genomic offset in conservation management. *Evolutionary Applications* **14**, 1202–1212 (2021).

30. L. Caproni, *et al.*, The genomic and bioclimatic characterization of Ethiopian barley (*Hordeum vulgare* L.) unveils challenges and opportunities to adapt to a changing climate. *Global Change Biology* gcb.16560 (2023). https://doi.org/10.1111/gcb.16560.

31. Á. J. Láruson, M. C. Fitzpatrick, S. R. Keller, B. C. Haller, K. E. Lotterhos, Seeing the Forest for the trees: Assessing genetic offset predictions from Gradient Forest. *Evolutionary Applications* 1–14 (2022). https://doi.org/10.1111/eva.13354.

32. O. B. Toon, *et al.*, Rapidly expanding nuclear arsenals in Pakistan and India portend regional and global catastrophe. *Sci. Adv.* **5**, eaay5478 (2019).

33. C. S. Harrison, *et al.*, A New Ocean State After Nuclear War. 1–19 (2022). https://doi.org/10.1029/2021AV000610.

34. T. Capblancq, B. R. Forester, Redundancy analysis: A Swiss Army Knife for landscape genomics. *Methods in Ecology and Evolution* **12**, 2298–2309 (2021).

35. L. Breiman, Random Forests. *Machine Learning* **45**, 5–32 (2001).

36. N. Ellis, S. J. Smith, C. Roland Pitcher, Gradient forests: Calculating importance gradients on physical predictors. *Ecology* **93**, 156–168 (2012).

37. J. A. Romero Navarro, *et al.*, A study of allelic diversity underlying flowering-time adaptation in maize landraces. *Nature Genetics* **49**, 476–480 (2017).

38. J. Bolaños, G. O. Edmeades, The importance of the anthesis-silking interval in breeding for drought tolerance in tropical maize. *Field Crops Research* **48**, 65–80 (1996).

39. C. G. Bardeen, *et al.*, Extreme Ozone Loss Following Nuclear War Results in Enhanced Surface Ultraviolet Radiation. *JGR Atmospheres* **126**, e2021JD035079 (2021).

40. P. Gienapp, *et al.*, Genomic Quantitative Genetics to Study Evolution in the Wild. *Trends in Ecology & Evolution* **32**, 897–908 (2017).

41. T. J. Kawecki, D. Ebert, Conceptual issues in local adaptation. *Ecology Letters* **7**, 1225–1241 (2004).

42. R. Leimu, M. Fischer, A Meta-Analysis of Local Adaptation in Plants. *PLoS ONE* **3**, e4010 (2008).

43. R. A. Bay, *et al.*, Genomic signals of selection predict climate-driven population declines in a migratory bird. *Science* **359**, 83–86 (2018).

44. S. Lachmuth, T. Capblancq, A. Prakash, S. R. Keller, M. C. Fitzpatrick, Novel genomic offset metrics integrate local adaptation into habitat suitability forecasts and inform assisted migration. *Ecological Monographs* **94**, e1593 (2024).

45. J. R. Lasky, M. B. Hooten, P. B. Adler, What processes must we understand to forecast regional-scale population dynamics? *Proceedings of the Royal Society B: Biological Sciences* **287**, 20202219 (2020).

46. Y. Vigouroux, *et al.*, Selection for Earlier Flowering Crop Associated with Climatic Variations in the Sahel. *PLoS ONE* **6**, e19563 (2011).

47. K. Dahal, X.-Q. Li, H. Tai, A. Creelman, B. Bizimungu, Improving Potato Stress Tolerance and Tuber Yield Under a Climate Change Scenario – A Current Overview. *Front. Plant Sci.* **10** (2019).

48. M. Jain, S. Naeem, B. Orlove, V. Modi, R. S. DeFries, Understanding the causes and consequences of differential decision-making in adaptation research: Adapting to a delayed monsoon onset in Gujarat, India. *Global Environmental Change* **31**, 98–109 (2015).

49. S. N. Aitken, M. C. Whitlock, Assisted Gene Flow to Facilitate Local Adaptation to Climate Change. *Annu. Rev. Ecol. Evol. Syst.* **44**, 367–388 (2013).

Figure legends

Figure 1 *Cycles* averaged simulated conditions for accessions projected to reach maturity, by soot scenario for A) barley B) maize C) rice subsp. *indica* D) rice subsp. *japonica* and E) sorghum. Lines are averaged across all simulated accessions of a species included in the model and colored by soot scenario. The vertical dotted line indicates the time of soot injection into the climate models. Control line indicates yearly fluctuations.

Figure 2 GF models capture current genotype-environment associations in maize landraces and were used to predict maladaptation under post-catastrophic climate scenarios. A) Phenotypic residuals (remining variation after accounting for experimental design) plotted against the GF offset of accessions grown in common gardens. GF offset is calculated for each phenotyped accession as the Euclidian distance of the expected genotype-environment relationship at a common garden common vs the genotype-environment relationship from the accessions' source location. Points with GF offset distance of zero indicate landrace accessions expected to be adapted to the common garden it was grown in. Yearly logged GF offset for B) maize C) barley D) rice subsp. *indica* E) rice subsp. *japonica* and F) Sorghum. Lines are averaged GF offset across all accessions of a species and colored by soot scenario. The dotted line indicates the time of soot injection into the climate models. Control line indicates yearly fluctuations maladaptation due to normal variability in climate. Inlayed scatter plots are the averaged logged GF offset across all accessions of a species two years after the incident.

Figure 3 Global distribution of logged GF offset, a measure of maladaptation, under the 150 Tg scenario 2, 9, and 16 years after the incident for landraces of the focal species A) barley B) maize C) rice subsp. *indica* D) rice subsp. *japonica* and E) sorghum. Higher GF offset values correspond to a larger degree of predicted maladaptation under the post-war scenario.

Figure 4 Substitution trajectories for the most vulnerable locations in year 2 of the 150 Tg scenario. For each crop, arrows connect the source location of landrace accession that is the most optimal to the vulnerable location (arrowhead) and are colored by the remaining GF offset (maladaptation) of the substitution. Substitutions are colored by how well-matched the moved landrace is to the vulnerable location, where colors corresponding to lower GF offset of substitution indicate a substitution that has a low degree of maladaptation to the novel environment. For each crop, substitution trajectories are provided for the most optimal substitution across all available germplasm and the best within country substitution.

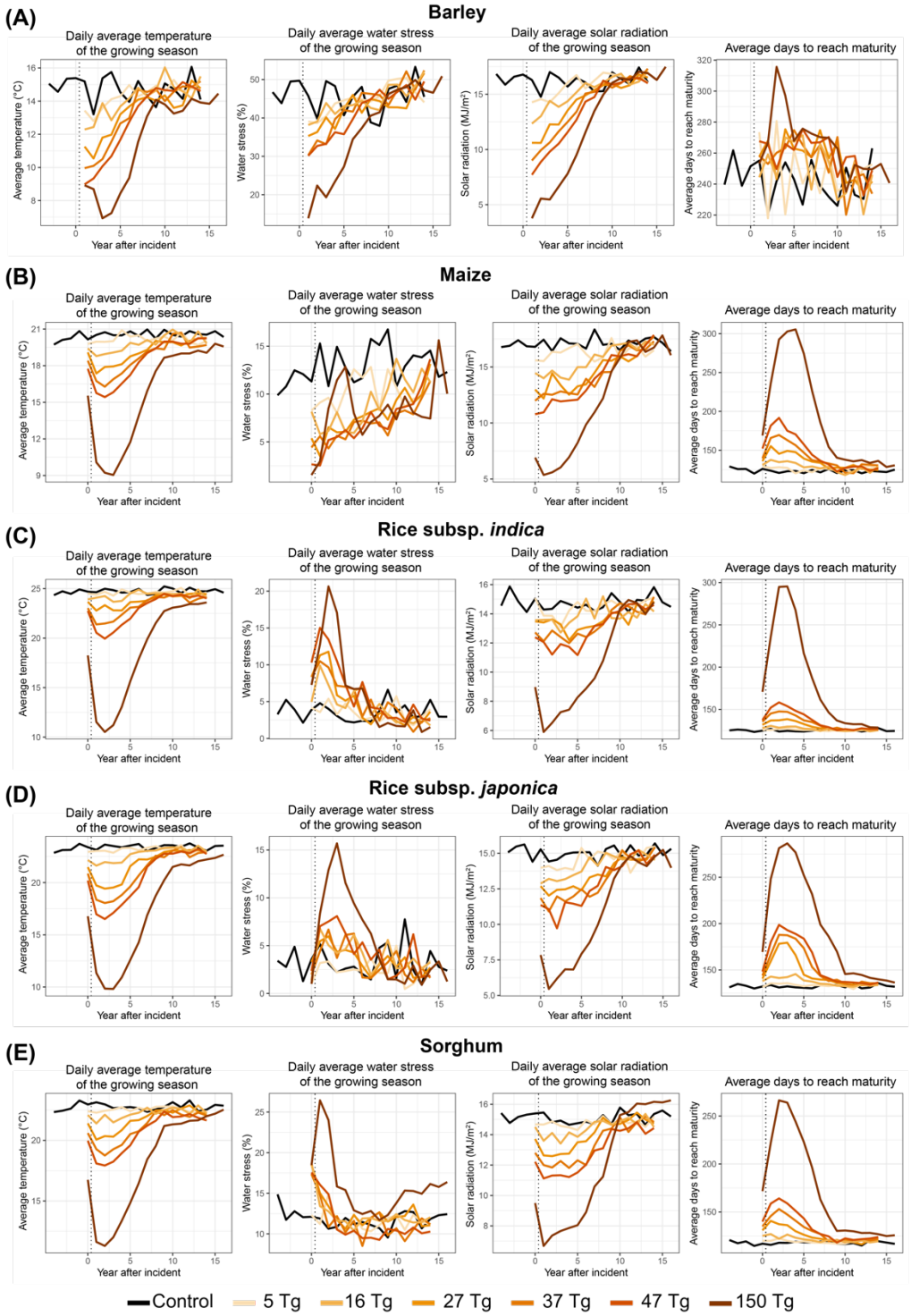

Figure 1 *Cycles* averaged simulated conditions for accessions projected to reach maturity, by soot scenario for A) barley B) maize C) rice subsp. *indica* D) rice subsp. *japonica* and E) sorghum. Lines are averaged across all simulated accessions of a species included in the model and colored by soot scenario. The vertical dotted line indicates the time of soot injection into the climate models. Control line indicates yearly fluctuations.

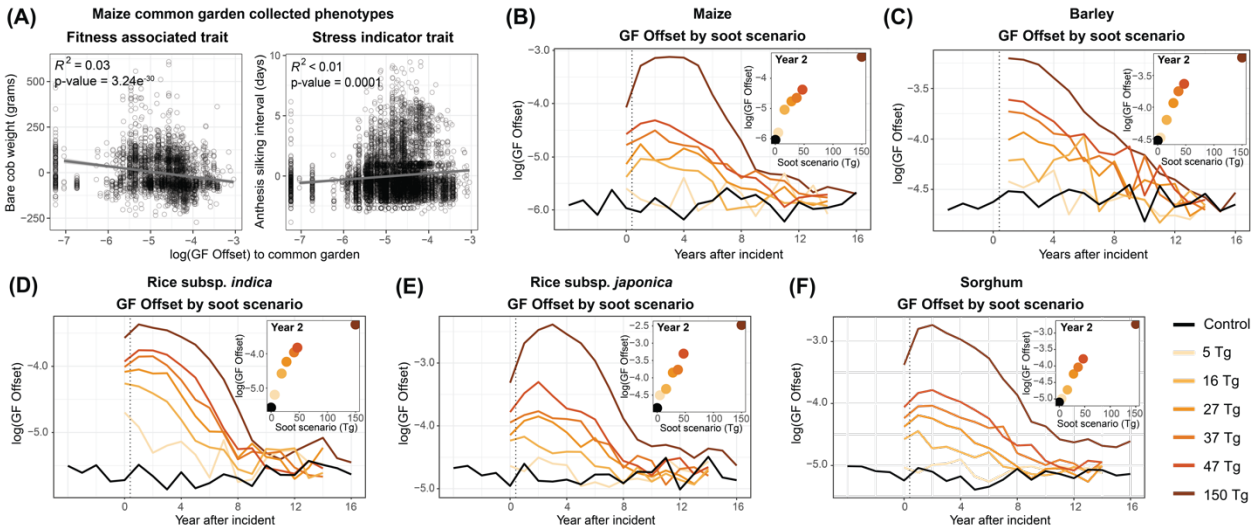

Figure 2 GF models capture current genotype-environment associations in maize landraces and were used to predict maladaptation under post-catastrophic climate scenarios. A) Phenotypic residuals (remining variation after accounting for experimental design) plotted against the GF offset of accessions grown in common gardens. GF offset is calculated for each phenotyped accession as the Euclidian distance of the expected genotype-environment relationship at a common garden common vs the genotype-environment relationship from the accessions' source location. Points with GF offset distance of zero indicate landrace accessions expected to be adapted to the common garden it was grown in. Yearly logged GF offset for B) maize C) barley D) rice subsp. *indica* E) rice subsp. *japonica* and F) Sorghum. Lines are averaged GF offset across all accessions of a species and colored by soot scenario. The dotted line indicates the time of soot injection into the climate models. Control line indicates yearly fluctuations maladaptation due to normal variability in climate. Inlayed scatter plots are the averaged logged GF offset across all accessions of a species two years after the incident.

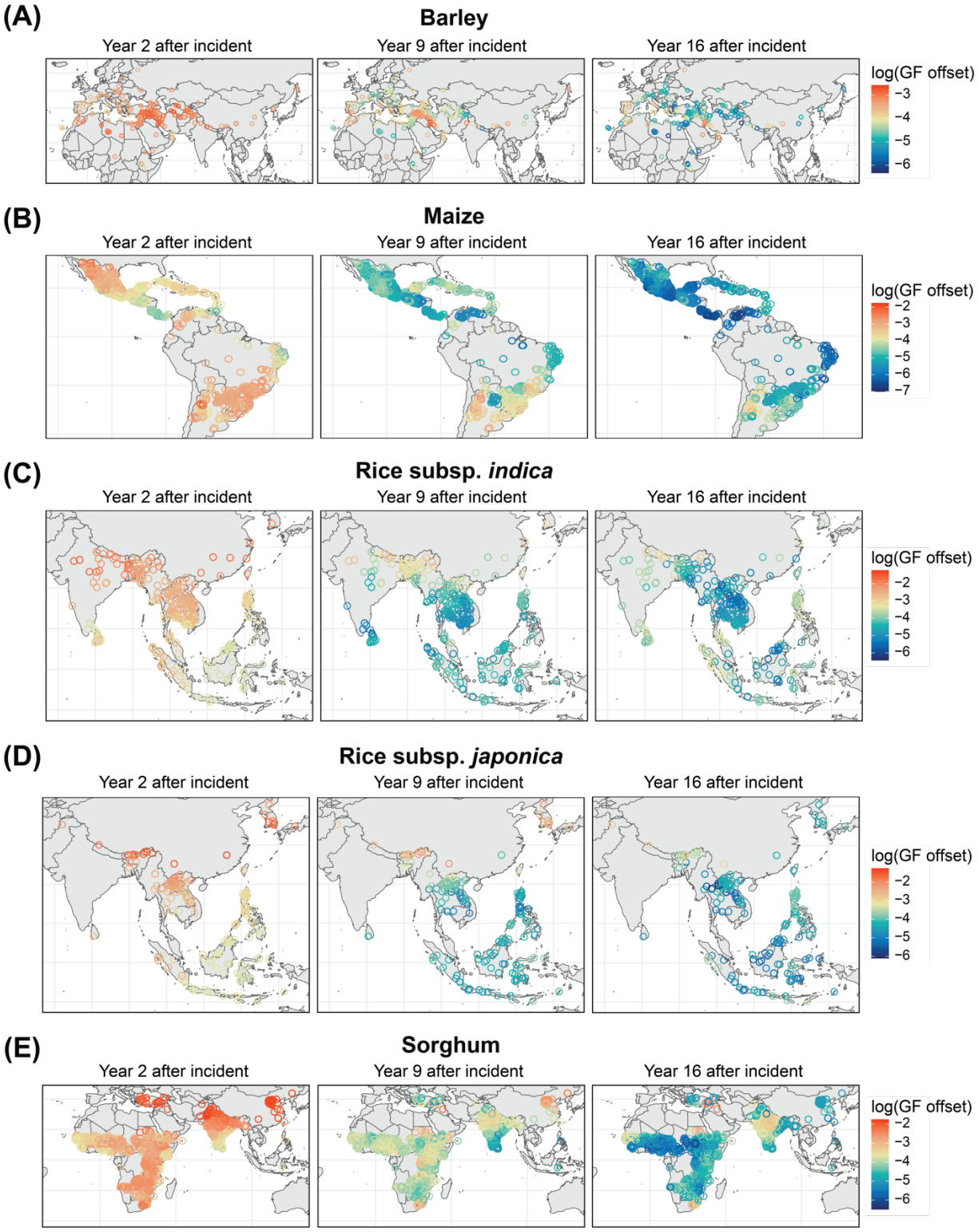

Figure 3 Global distribution of logged GF offset, a measure of maladaptation, under the 150 Tg scenario 2, 9, and 16 years after the incident for landraces of the focal species A) barley B) maize C) rice subsp. *indica* D) rice subsp. *japonica* and E) sorghum. Higher GF offset values correspond to a larger degree of predicted maladaptation under the post-war scenario.

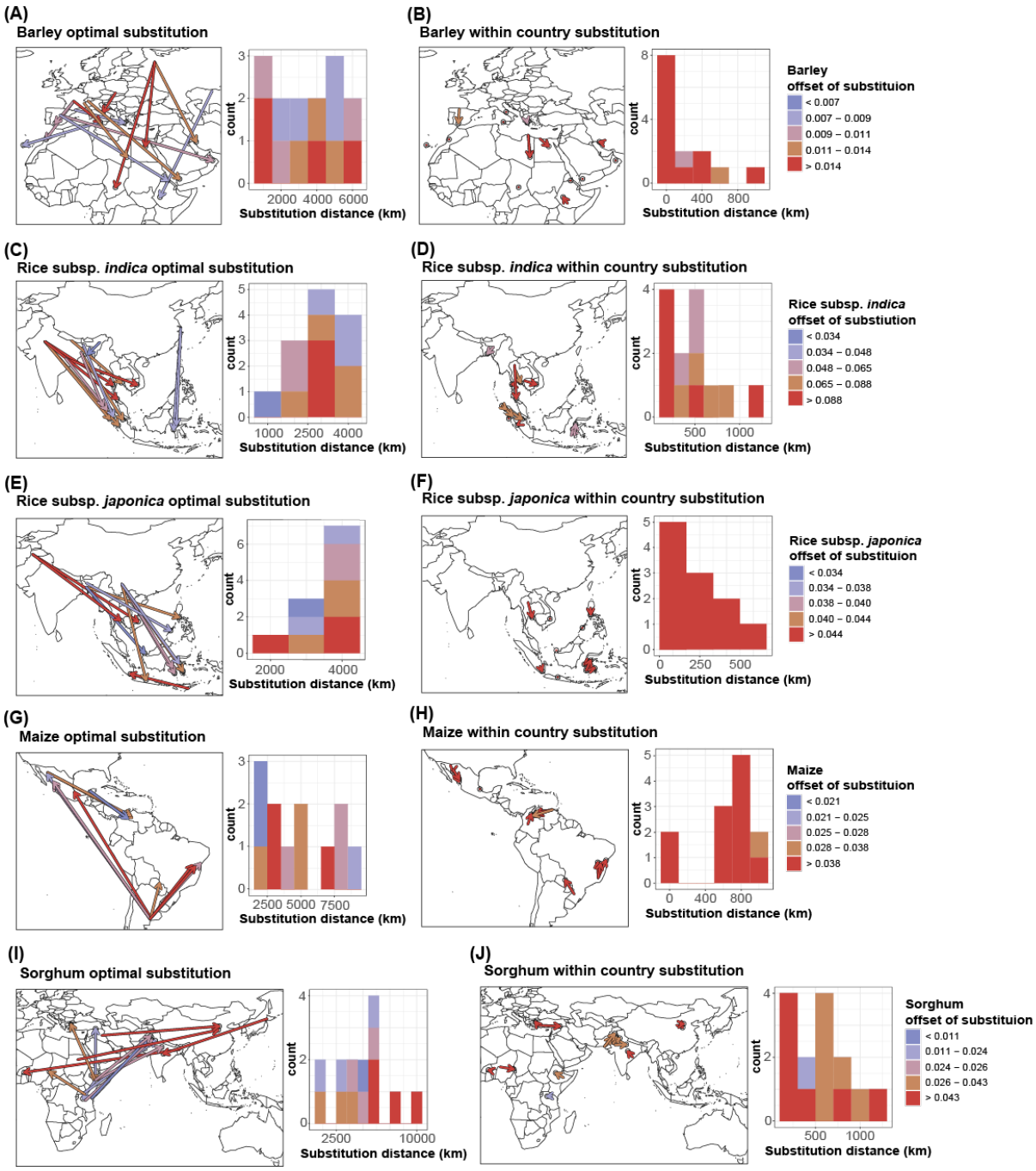

Figure 4 Substitution trajectories for the most vulnerable locations in year 2 of the 150 Tg scenario. For each crop, arrows connect the source location of landrace accession that is the most optimal to the vulnerable location (arrowhead) and are colored by the remaining GF offset (maladaptation) of the substitution. Substitutions are colored by how well-matched the moved landrace is to the vulnerable location, where colors corresponding to lower GF offset of substitution indicate a substitution that has a low degree of maladaptation to the novel environment. For each crop, substitution trajectories are provided for the most optimal substitution across all available germplasm and the best within country substitution.